ADVANCED MATERIALS

Supporting Information

for *Adv. Mater.*, DOI: 10.1002/adma.201201364

On-Demand Separation of Oil-Water Mixtures

*Gibum Kwon, Arun. K. Kota, Yongxin Li, Ameya Sohani, Joseph M. Mabry, and Anish Tuteja**

Submitted to ADVANCED MATERIALS

Supporting Information for *On-demand* Separation of Oil-Water Mixtures

By *Gibum Kwon, Arun. K. Kota, Yongxin, Li, Ameya Sohani, Joseph M. Mabry,* and *Anish Tuteja**

[*] Prof. A. Tuteja, Gibum Kwon, Dr. Arun K. Kota, Yongxin Li, Ameya Sohani
Department of Materials Science and Engineering
University of Michigan, Ann Arbor, MI, 48109 (USA)
E-mail: atuteja@umich.edu
Dr. J. M. Mabry
Space and Missile Propulsion Division
Air Force Research Laboratory, Edwards Air Force Base, CA, 93524 (USA)

Section 1. Derivation of the critical pressure $P_{critical}$ and the estimated values for $P_{critical}$.

Consider a liquid in the Cassie-Baxter state on a textured surface composed of periodic, non-woven cylindrical fibers with radius *R* and half inter-fiber spacing *D* (see Fig. 1f in the main manuscript). The liquid-air interface is located at a local texture angle ψ of the re-entrant texture with a sagging angle $\delta\theta = \theta - \psi$, as shown in Fig. 1f of the main manuscript. A force balance between the applied pressure $P_{applied}$ on a droplet and the surface tension γ_{12} can be written as:

$$P_{applied} \cdot (interfacial\ area) = \gamma_{12} \cdot (contact\ line length) \cdot \sin\delta\theta \quad \text{(S1)}$$

For cylindrical fibers of length *L*, Eq. S1 becomes:

$$P_{applied} \cdot L \cdot 2(D + R - R\sin\psi) = \gamma_{12} \cdot 2L \cdot \sin\delta\theta \quad \text{(S2)}$$

Simplifying Eq. S2, we get:

$$P_{applied} = \frac{\gamma_{12}\sin(\theta - \psi)}{D + R - R\sin\psi} \quad \text{(S3)}$$

For a given liquid and re-entrant texture geometry, Eq. S3 indicates that the applied pressure $P_{applied}$ determines the local texture angle ψ, where the liquid forms a stable composite interface. We determine the critical texture angle ψ_{cr}, which corresponds to the maximum pressure $P_{critical}$ that the liquid-air interface can withstand by solving:

$$\frac{dP_{applied}}{d\psi} = 0 \text{ with } \frac{d^2P_{applied}}{d\psi^2} < 0 \text{ at } \psi = \psi_{cr} \quad \text{(S4)}$$

From Eqs. S3 and S4 we obtain,

$$(D + R - R\sin\psi_{cr}) \cdot (-\cos(\theta - \psi_{cr})) - \sin(\theta - \psi_{cr}) \cdot (-R\cos\psi_{cr}) = 0$$

$$\Rightarrow (D + R) \cdot \cos(\theta - \psi_{cr}) - R\sin\theta = 0$$

Simplifying further, we obtain,

$$P_{critical} = \frac{\gamma_{12}\sin(\theta - \psi_{cr})}{D + R - R\sin\psi_{cr}}, \text{where } \psi_{cr} = \theta - \cos^{-1}\left(\frac{R\sin\theta}{R+D}\right) \quad \text{(S5)}$$

When $P_{applied} > P_{critical}$, the liquid-air interface spontaneously advances downwards (i.e., to $\psi < \psi_{cr}$) and the liquid transitions to the Wenzel state.

Table S1 shows the values of $P_{critical}$ for water and hexadecane, with and without surfactants, on the dip-coated nylon membranes (R = 20.3 μm, $2D$ = 28 μm). The estimation of the Young's[1] contact angle θ is discussed in supporting information section 3. We estimated the surface tensions γ_{12} for water and hexadecane with surfactants using the capillary rise method.[2]

Table S1. Calculated values of $P_{critical}$ for water and hexadecane on the dip-coated nylon membranes (R = 20.3 μm, $2D$ = 28 μm), with and without surfactants.

	θ ($\theta_{adv}, \theta_{rec}$)	γ_{12} (mN m^{-1})	ψ_{cr}	$P_{critical}$ (Pa)
Water	115° (122°, 109°)	72.1	57.4°	3540
Water with 1.2 mg mL^{-1} PS80	79° (95°, 65°)	40.2	24.5°	1265
Hexadecane	72° (77°, 68°)	27.5	16.3°	794
Hexadecane with 0.3 mg mL^{-1} PS80	68° (75°, 61°)	24.9	11.3°	686
Hexadecane with 1.4 mg mL^{-1} span80	68° (76°, 61°)	25.7	11.3°	708

Section 2. Electric field driven Cassie-Baxter to Wenzel transition.

Consider a polar liquid column in the Cassie-Baxter state on the membrane module used in this work (see the schematic inset in Fig. 1g of the main manuscript). The membrane module consists of a stack of three dip-coated nylon membranes and an electrode, as shown by the schematic in Fig. S1. When an electric field is applied across the electrode and the polar liquid column on the textured substrate, a Maxwell stress $P_{Maxwell} = \varepsilon_o\varepsilon_d V^2 / 2t_{eff}^2$ (with parallel plate capacitor assumption) is exerted on the liquid-air interface.[3, 4] When the liquid-air interface is located at $\psi = \psi_{cr}$ on the first layer of texture (i.e., the top dip-coated nylon membrane), t_{eff} is given as (see Fig. S1):

$$t_{eff} = 6R - R(1 + \cos\psi_{cr}) - R_{sag,cr}\left[1 - \cos(\theta - \psi_{cr})\right] \quad \text{(S6)}$$

Here, $R_{sag,cr} = \left(D + R - R\sin\psi_{cr}\right)/\sin\left(\theta - \psi_{cr}\right)$ is the critical radius of curvature of the liquid-air interface. Using Eq. S6, we estimate t_{eff} = 81.1 μm for water and t_{eff} = 69.7 μm for water with 1.2 mg mL^{-1} of PS80.

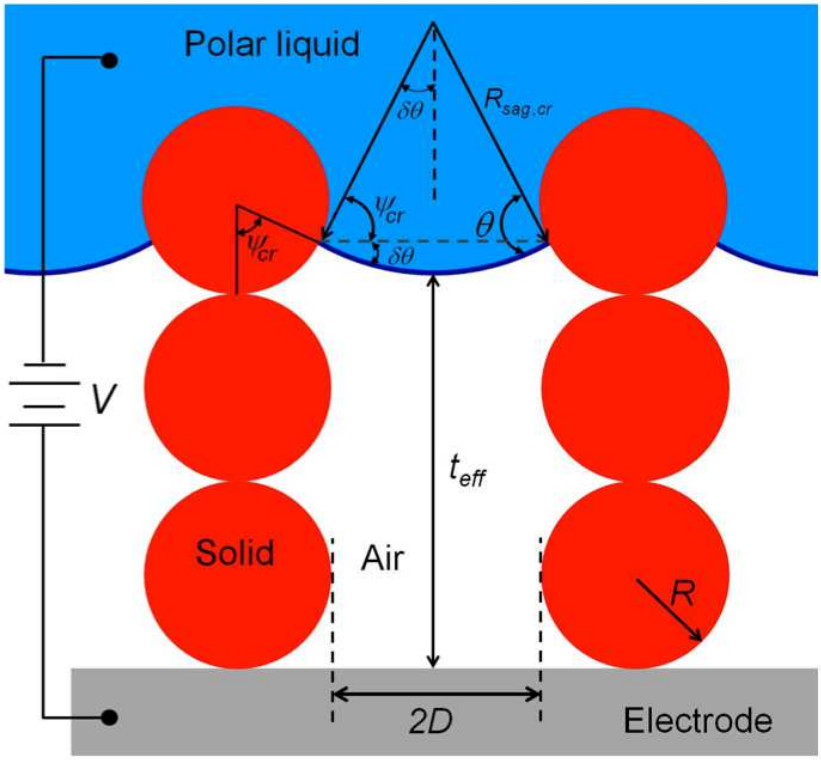

Figure S1. A schematic showing the pressure-induced sagging of the liquid-air interface on a stack of three membranes with cylindrical texture.

The liquid-air interface can withstand the maximum pressure $P_{critical}$ when it is located at $\psi = \psi_{cr}$ (see supporting information section 1). If the applied voltage *V* is such that $P_{applied} = \left(P_{hydrostatic} + P_{Maxwell}\right) > P_{critical}$, the liquid-air interface spontaneously advances downwards (i.e., to $\psi < \psi_{cr}$) until it reaches the bottom of the first layer of texture. At the same applied voltage *V*, the liquid cannot form a stable composite interface on subsequent layers of the texture (i.e., the middle or the bottom dip-coated nylon membranes) because $P_{Maxwell}$ is amplified due to a decrease in t_{eff} , which leads to an increase in $P_{applied}$. Consequently, once the liquid-air interface advances past $\psi = \psi_{cr}$ on the first layer of texture, the liquid transitions from the Cassie-Baxter state to the Wenzel state.

Note that the above analysis assumes a geometry similar to a parallel plate capacitor. Our experimental observations for the permeation of water (or the water-rich phase) through the membrane, i.e., transition from the Cassie-Baxter state to the Wenzel state, match well with the predictions based on the above analysis (see main manuscript). However, it should be noted that the parallel plate capacitor assumption might not be valid for all real systems, in

which case the analysis for the Cassie-Baxter to Wenzel transition can be significantly more complex.

Section 3. Estimation of the Young's contact angle.

While the advancing contact angle θ_{adv} and receding contact angle θ_{rec} are readily measurable quantities, the Young's[1] contact angle θ is not a measurable quantity. However, it can be estimated from θ_{adv} and θ_{rec} as:[5]

$$\theta = \cos^{-1}\left(\frac{\Gamma_{adv}\cos\theta_{adv} + \Gamma_{rec}\cos\theta_{rec}}{\Gamma_{adv} + \Gamma_{rec}}\right) \tag{S7}$$

where,

$$\Gamma_{adv} = \left(\frac{\sin^3\theta_{adv}}{2 - 3\cos\theta_{adv} + \cos^3\theta_{adv}}\right)^{1/3} \tag{S8}$$

and

$$\Gamma_{rec} = \left(\frac{\sin^3\theta_{rec}}{2 - 3\cos\theta_{rec} + \cos^3\theta_{rec}}\right)^{1/3} \tag{S9}$$

The measured advancing and receding contact angles, and the estimated Young's contact angles for water and hexadecane, with and without surfactants, on surfaces spin-coated with 50 wt% fluorodecyl POSS + x-PDMS blend are listed in Table S1.

Section 4. Size distribution of the dispersed phase in the emulsions.

Surfactant stabilized mixtures of oil and water are classified based on the diameter of the dispersed phase. A mixture is considered free oil and water if the diameter > 150 μm, a dispersion if the diameter is between 20 μm and 150 μm, and an emulsion if the diameter < 20 μm.[6] We determined the size distributions of the dispersed phase in the emulsions using two techniques – optical microscopy image analysis (Olympus BH-2 optical microscope and ImageJ software) for droplets above 1 μm in diameter and dynamic light scattering (DLS, Malvern Zetasizer Nano ZS instrument) for droplets below 1 μm.

Figs. S2a and S2d show representative optical microscopy images for the 50:50 vol:vol polysorbate80 stabilized hexadecane-in-water and the 30:70 vol:vol span80 stabilized water-in-hexadecane feed emulsions, respectively. Ten different images with more than 100 drops per image were analyzed to reduce the error in the estimated size distribution. Figs. S2b and S2e show the number size distributions of the dispersed phase determined using image analysis, in hexadecane-in-water and water-in-hexadecane feed emulsions, respectively. The average size of dispersed phase for both the hexadecane-in-water and water-in-hexadecane feed emulsions is between 10–20 μm. Figs. S2c and S2f show the number size distributions of

the dispersed phase determined using DLS, for hexadecane-in-water and water-in-hexadecane feed emulsions, respectively. The size of dispersed phase in hexadecane-in-water feed emulsions is between 200-300 nm, while that in water-in-hexadecane feed emulsion is between 200-400 nm.

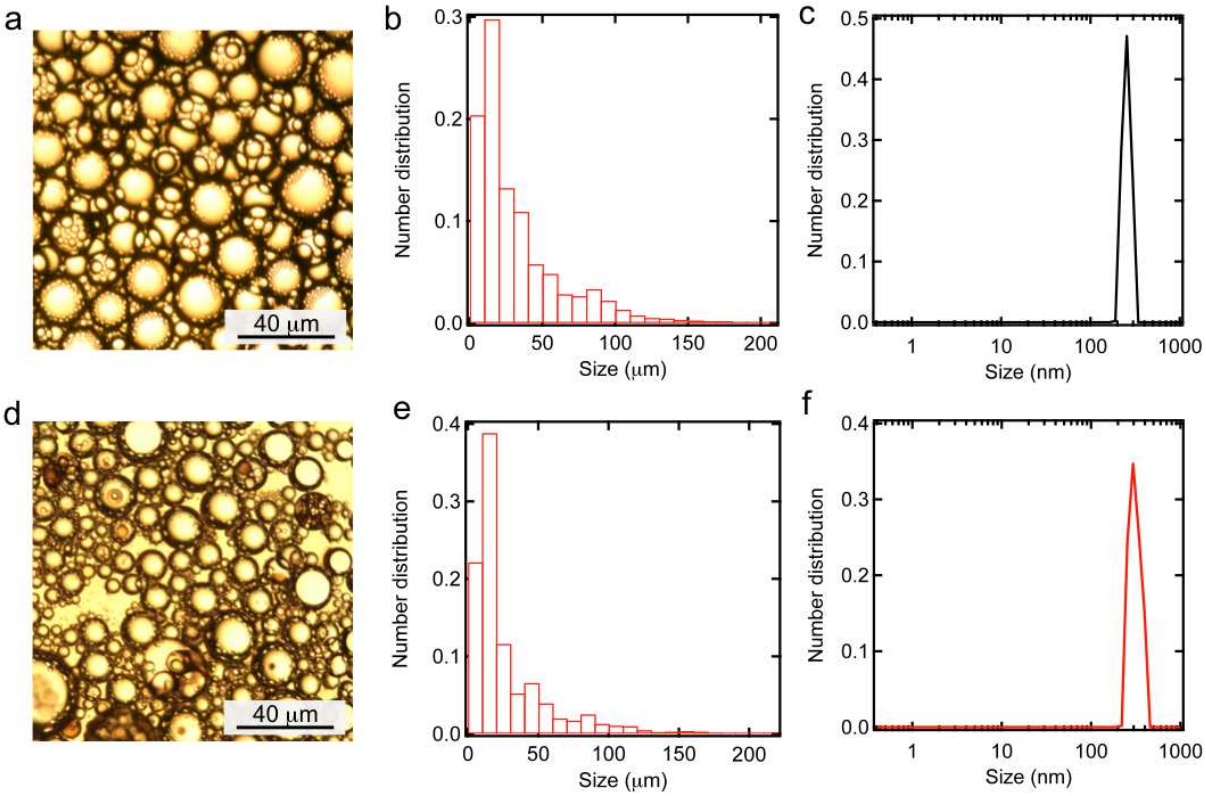

Figure S2. a) A representative optical microscopy image of the hexadecane-in-water feed emulsion. b) and c) The number size distributions for the hexadecane-in-water feed emulsion for droplets > 1 μm and < 1 μm, respectively. d) A representative optical microscopy image of the water-in-hexadecane feed emulsion. e) and f) The number size distributions for the water-in-hexadecane feed emulsion for droplets > 1 μm and < 1 μm, respectively.

Fig. S3a shows the number size distribution for the permeate obtained from the separation of a hexadecane-in-water emulsion determined using image analysis. The average size of dispersed phase in the permeate is between 10–20 μm. Comparing hexadecane-in-water feed emulsion with the permeate, it is evident that nearly all hexadecane droplets above 30 μm were removed during separation. Fig. S3b shows the number size distribution for the permeate obtained from separation of hexadecane-in-water emulsion determined by using DLS. The size of dispersed phase in the permeate is between 200–300 nm. Comparing the hexadecane-in-water feed emulsion with the permeate, it is evident that the droplet size distribution below 1 μm remains unchanged during separation.

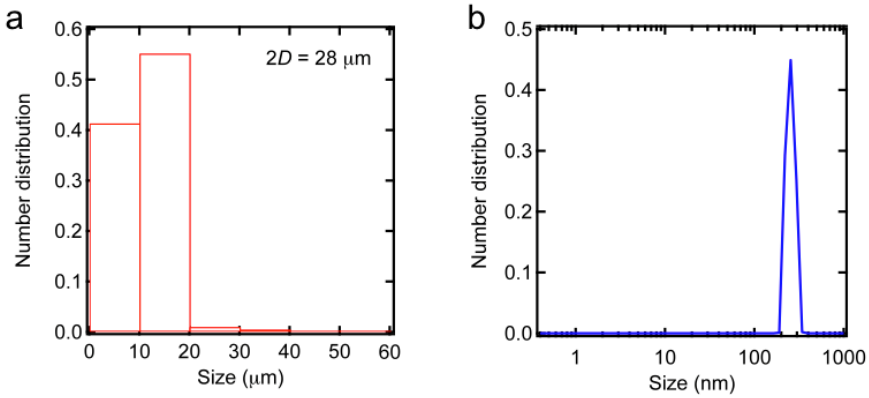

Figure S3. a) and b) The number size distributions of the permeate from the separation of the hexadecane-in-water emulsion obtained with optical image analysis and DLS, respectively.

Section 5. Competitive wetting of water and hexadecane in the presence of PS80.

In the case of hexadecane-in-water emulsions, the medium surrounding the emulsified hexadecane droplets is water. In order to study the wetting behavior of hexadecane surrounded by water upon applying an electric field, we conducted EWOD of a hexadecane droplet on a non-textured 50 wt% fluorodecyl POSS + x-PDMS substrate submerged in water, in the presence of PS80. Fig. S4a shows the macroscopic contact angles for hexadecane as a function of the voltage V applied across the dielectric layer. In contrast to the behavior observed in Figs. 1a and 2a in the main manuscript, the macroscopic contact angle for hexadecane *increases* from $\theta^{ew}_{hexadecane}$ = 58º at V = 0 V (see inset (i) in Fig. S4a) until it saturates at $\theta^{ew}_{hexadecane}$ = 115º (see inset (ii) in Fig. S4a). This is a direct consequence of the decrease in the macroscopic contact angle for water,[7, 8] $\theta^{ew}_{water} = \pi - \theta^{ew}_{hexadecane}$, as shown in Fig. S4b. The macroscopic contact angle for water decreases from θ^{ew}_{water} = 122º at V = 0 V until it saturates at θ^{ew}_{water} = 65º, and this manifests as an increase in the macroscopic contact angle for hexadecane. For ε_d = 1.9 (as was the case for the data shown in Figs. 1a and 2a in the main manuscript) and oil-water interfacial tension γ_{ow} = 8.1 mN m^{-1}, the predictions from Young-Lippmann equation (see Eq. 1 in the main manuscript) match well with experimental data for water.

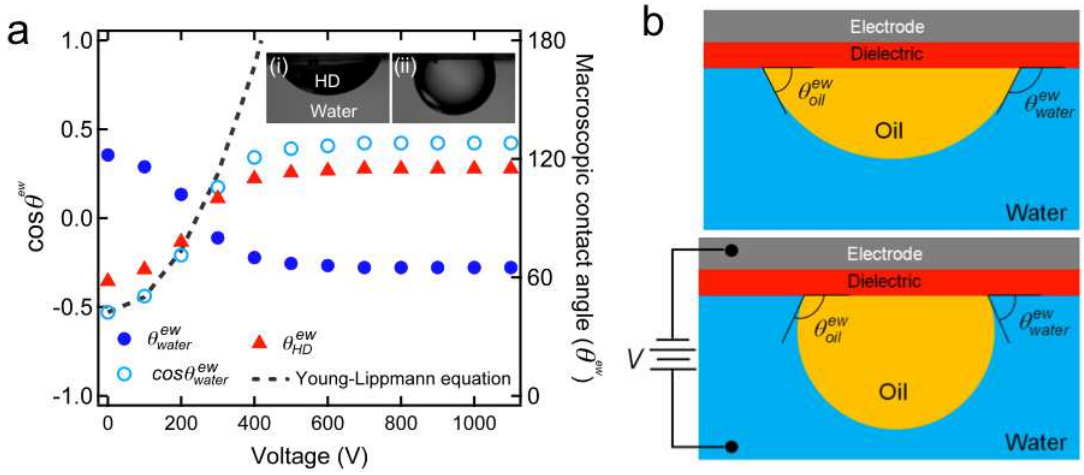

Figure S4. a) Competitive wetting of water and hexadecane containing PS80. The insets (i) and (ii) show the macroscopic contact angle for hexadecane before and after applying voltage, respectively. b) A schematic illustrating the competitive wetting of water and oil. The sum of the macroscopic contact angles for water and oil is 180°.

We estimated the interfacial tension γ_{ow} between water and hexadecane in the presence of PS80 by using the relationship postulated by Fowkes:[9]

$$\gamma_{ow} = \gamma_{ov} + \gamma_{wv} - 2\sqrt{\gamma_{ov}^{d}\gamma_{wv}^{d}} \quad \text{(S10)}$$

Here, γ_{ow} is the hexadecane-water interfacial tension. γ_{ov} and γ_{wv} are the surface tensions, while γ_{ov}^{d} and γ_{wv}^{d} are the dispersive components of the surface tensions for hexadecane and water, respectively. Note that $\gamma_{ov} = \gamma_{ov}^{d}$ for hexadecane (non-polar liquid). Using the capillary rise method,[2] we determined γ_{ov} = 24.9 mN m^{-1} with 0.3 mg mL^{-1} of PS80 and γ_{wv} = 40.2 mN m^{-1} with 1.2 mg mL^{-1} of PS80. In order to estimate γ_{wv}^{d}, we combined the Young's equation[1] with the relationship postulated by Fowkes[9] for the interfacial tension of a non-polar solid (such as a 50 wt% fluorodecyl POSS + x-PDMS blend) and water to obtain:

$$\gamma_{wv}^{d} = \frac{\gamma_{wv}(1+\cos\theta)}{4\gamma_{sv}^{d}} \quad \text{(S11)}$$

Here, γ_{sv}^{d} is the dispersive component of the solid surface energy and θ is the Young's contact angle for water. On a spin-coated surface of 50 wt% fluorodecyl POSS + x-PDMS, the contact angles for water with 1.2 mg mL^{-1} of PS80 is θ_{water} = 95°. Using this value in Eq. S11, we obtained γ_{wv}^{d} = 32.6 mN m^{-1} for water with 1.2 mg mL^{-1} of PS80. Substituting the values of γ_{ov}, γ_{wv} and γ_{wv}^{d} in Eq. S10, we determined γ_{ow} = 8.1 mN m^{-1} in the presence of PS80.

Section 6. Methods to estimate separation efficiency.

We used the following three techniques to estimate the separation efficiency of our oil-water emulsion separation methodology:

A. Thermogravimetric Analysis (TGA):

We determined the composition of the hexadecane-rich and the water-rich phases after separation using TGA (Perkin Elmer Pyris 1 TGA). Approximately 50 mg of the sample was heated from room temperature to 105°C at a rate of 5°C s^{-1}, and the temperature was held constant at 105°C for 60 minutes. Note that the boiling point of hexadecane is 287ºC. The loss in weight of water was used to estimate the purity of the water-rich phase. The loss in weight of the hexadecane-rich phase was compared with the loss in weight of the as-obtained hexadecane to estimate the purity of the hexadecane-rich phase. Fig. S5a shows the data for the hexadecane-rich retentates and the water-rich permeates obtained from the batch separation of both the hexadecane-in-water emulsions and the water-in-hexadecane emulsions. The data for pure water and as-obtained hexadecane (HD) are also shown for comparison. The measurements show that the permeates contain ~ 0.1 wt% of hexadecane while the retentates contain ~ 0.1 wt% of water.

B. Transmittance measurements:

We conducted transmittance measurements using a Cary 50 Bio UV-vis spectrophotometer to estimate the permeate (water-rich phase) quality relative to the feed emulsions. Fig. S5b shows the transmittance of hexadecane-in-water and water-in-hexadecane feed emulsions (absorbance normalized to 1), the transmittance of the corresponding permeates, as well as, the transmittance of pure water between 390 nm and 750 nm (visible spectrum). It is evident that both the feed emulsions are very turbid, while the corresponding permeates are very clear. This indicates that our separation methodology leads to nearly complete separation.

C. Karl Fischer Analysis:

Karl Fischer analysis is widely used to estimate water content in various oils.[10, 11] The water content in the hexadecane-rich phase was determined by injecting samples ranging from 10 μL to 0.6 mL into an EM Science AquaStar C3000 Titrator for coulometric Karl Fischer titration analysis (ASTM D6304). The hexadecane-rich permeate from the continuous separation of water-in-hexadecane emulsion contained ~ 88 ppm water (i.e., ~ 0.0088 wt% water). Note that the solubility of water in hexadecane at room temperature is ~ 20-50 ppm.[12, 13]

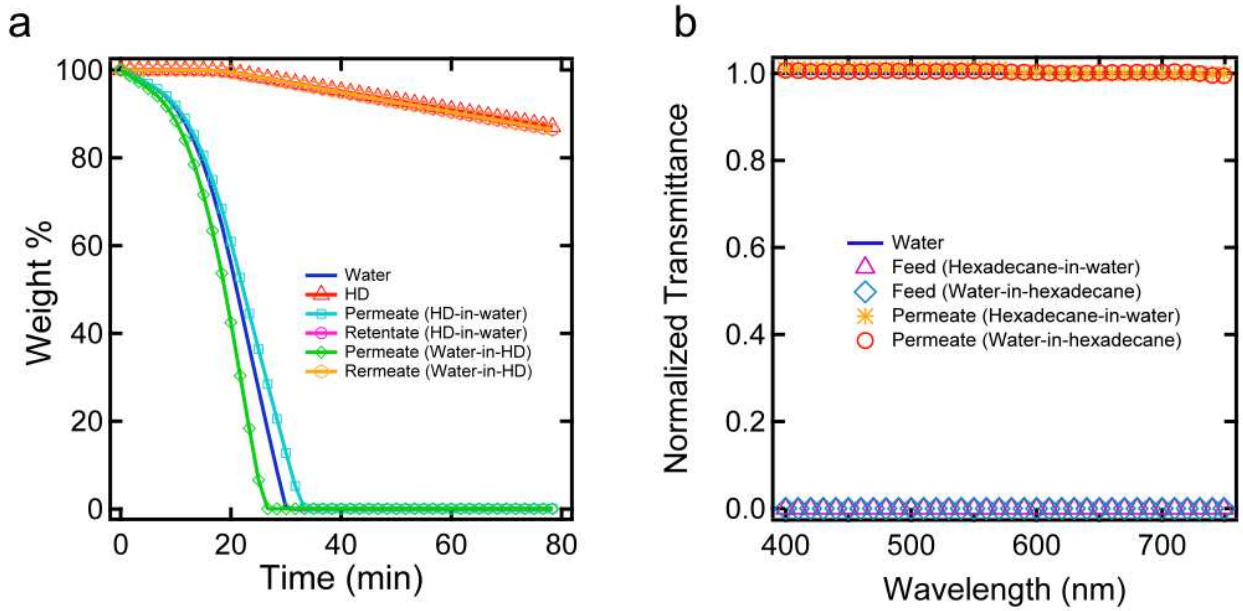

Figure S5. a) TGA data for the permeates and the retentates obtained from the batch separation of hexadecane-in-water and water-in-hexadecane emulsions. b) Transmittance data for hexadecane-in-water feed emulsion, water-in-hexadecane feed emulsion, and the corresponding permeates after separation.

Section 7. Location and concentration of the surfactant after oil-water emulsion separation

We estimated the amount of surfactant in the permeate and the retentate after emulsion separation by measuring the permeate and retentate contact angles and comparing them with calibration curves of contact angles for water and hexadecane as a function of surfactant concentration. The calibration curves were developed by measuring the contact angles on flat surfaces spin-coated with a 50 wt% fluorodecyl POSS + x-PDMS blend. The 50 wt% fluorodecyl POSS + x-PDMS blend was chosen because it is essentially non-polar.

Figs. S6a and S6b show the advancing and receding contact angles for water and hexadecane, respectively, as a function of PS80 concentration. After the batch separation of PS80 stabilized hexadecane-in-water emulsion, the advancing and receding contact angles for the water-rich permeate are 94º ± 2º and 64º ± 2º while those of hexadecane-rich retentate are 76º ± 2º and 63º ± 2º. By comparing these values with Figs. S6a and S6b, it is evident that the concentration of PS80 in the water-rich permeate is between 1.2-1.5 mg mL^{-1} and the concentration of PS80 in the hexadecane-rich retentate is 0-0.3 mg mL^{-1}. This is because of the higher solubility of PS80 in water when compared to hexadecane.

In contrast to PS80, span80 is virtually insoluble in water. The advancing and receding contact angles for the water-rich permeates from the batch separation and the continuous separation of water-in-hexadecane emulsions are 123°±2° and 108°±2°, respectively. By comparing these values with those of water without any surfactant (see Table S1), it is evident

that there is no span80 in the water-rich phase. Consequently, after separation of the water-in-hexadecane emulsions, we estimate that nearly all the span80 is in the hexadecane-rich phase.

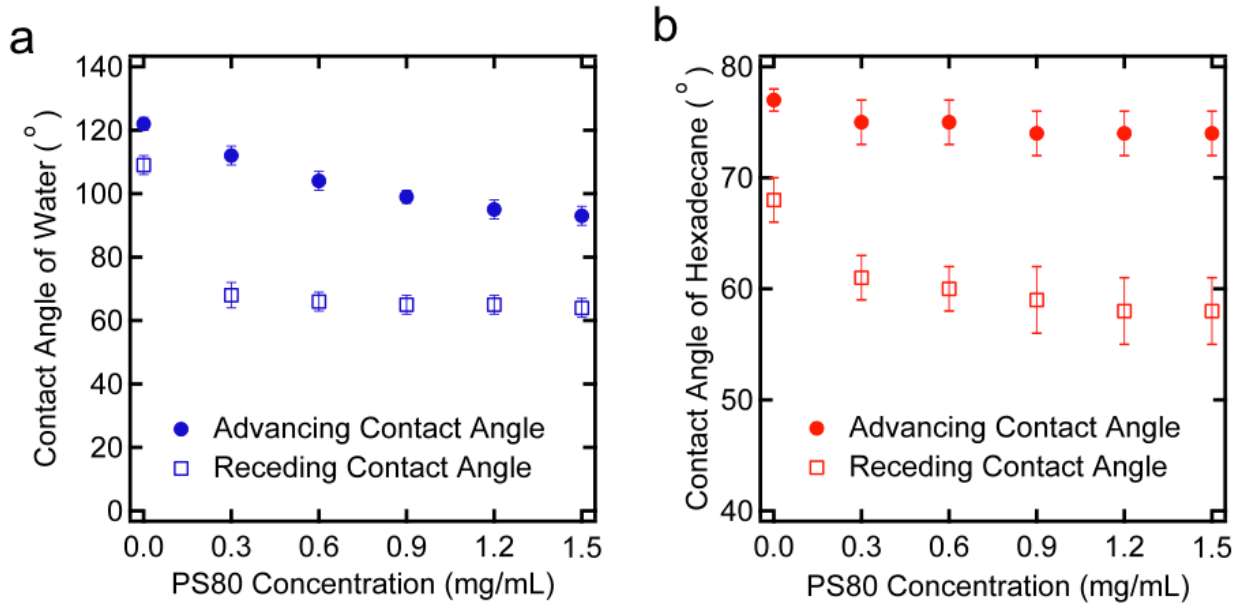

Figure S6. a) and b) The advancing and receding contact angles for water and hexadecane, respectively, as a function of PS80 concentration.

Section 8. Fraction of emulsified water droplets removed from water-in-hexadecane feed emulsions.

100 mL of 30:70 vol:vol water-in-hexadecane feed emulsion contains 30 mL of water and 70 mL of hexadecane. We determined the volume fraction of emulsified water droplets (< 20 μm) in our feed emulsions to be 0.016 from the volume size distribution (see Fig. S7). Thus, the volume of emulsified water droplets in 100 mL of feed emulsion is 0.48 mL. In continuous separation, 100 mL of feed emulsion results in approximately 30 mL of water-rich permeate and 70 mL of hexadecane-rich permeate. Karl Fischer analysis (see supporting information section 6) indicates that the amount of water in the hexadecane-rich permeate is ~ 0.0088 wt%, which is equivalent to ~ 0.0068 vol%. Thus, the volume of water in the hexadecane-rich permeate is 0.0047 mL. Even if we assume that the size of all the water droplets in the hexadecane-rich permeate is < 20 μm, comparing the volume of the emulsified water droplets in the feed emulsion (0.48 mL) to that in the hexadecane-rich permeate (0.0047 mL), we conclude that the volumetric fraction of emulsified droplets removed during separation is at least 99%.

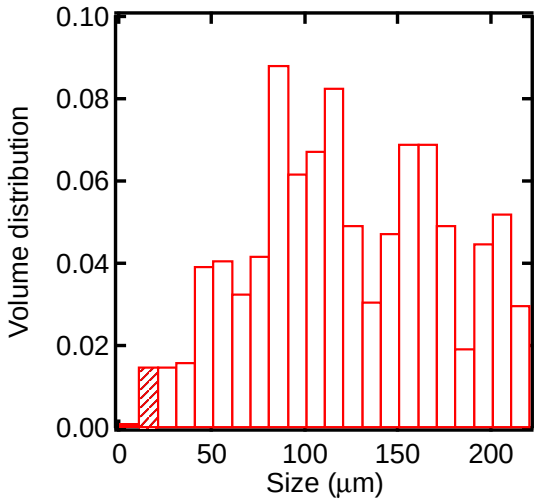

Figure S7. Volume size distribution of water droplets for the water-in-hexadecane feed emulsion. The dashed region represents droplets below 20 μm (emulsified droplets).

References:

[1] T. Young, *Philos. T. R. Soc. Lond.* **1805**, *95*, 65.
[2] G. K. Batchelor, *An introduction in fluid dynamics*, Cambridge University Press, London, UK **1970**.
[3] G. Manukyan, J. M. Oh, D. van den Ende, R. G. H. Lammertink, F. Mugele, *Phys. Rev. Lett.* **2011**, *106*.
[4] J. M. Oh, G. Manukyan, D. van den Ende, F. Mugele, *Europhys. Lett.* **2011**, *93*.
[5] R. Tadmor, *Langmuir* **2004**, *20*, 7659.
[6] M. Cheryan, N. Rajagopalan, *J. Membrane Sci.* **1998**, *151*, 13.
[7] M. S. Dhindsa, N. R. Smith, J. Heikenfeld, P. D. Rack, J. D. Fowlkes, M. J. Doktycz, A. V. Melechko, M. L. Simpson, *Langmuir* **2006**, *22*, 9030.
[8] B. Janocha, H. Bauser, C. Oehr, H. Brunner, W. Gopel, *Langmuir* **2000**, *16*, 3349.
[9] F. M. Fowkes, *Ind. Eng. Chem.* **1964**, *56*, 40.
[10] M. Garcia-Perez, S. Wang, J. Shen, M. Rhodes, W. J. Lee, C. Z. Li, *Energ. Fuel.* **2008**, *22*, 2022.
[11] S. A. Margolis, *Anal. Chem.* **1995**, *67*, 4239.
[12] P. Schatzberg, *J. Phys. Chem.* **1963**, *67*, 776.
[13] Schatzberg.P, *J. Polym. Sci. Pol. Sym.* **1965**, 87.

Movie Legends

Movie S1. This video demonstrates the *on-demand* separation of free oil (hexadecane) and water driven by gravity. A liquid column of hexadecane (dyed red) and water (dyed blue) is retained above the membrane before applying an electric field. When a voltage $V \approx 2.0$ kV is applied, water permeates through while hexadecane is retained above the membrane.

Movie S2. This video demonstrates the *on-demand* separation of PS80 stabilized hexadecane-in-water emulsion driven by gravity. A liquid column of hexadecane-in-water emulsion is retained above the membrane before applying an electric field. When a voltage $V \approx 1.1$ kV is applied, the water-rich permeate passes through, while hexadecane-rich retentate is retained above the membrane. Water is dyed blue and hexadecane is dyed red.

Movie S3. This video demonstrates the *on-demand* separation of PS80 stabilized hexadecane-in-water emulsion using the scaled-up apparatus. The dip-coating based membrane module is easy to scale-up, and allows for the separation of larger quantities of hexadecane-in-water emulsions. When a voltage $V \approx 1.1$ kV is applied, the water-rich permeate passes through while hexadecane-rich retentate is retained above the membrane. Water is dyed blue and hexadecane is dyed red.

Movie S4. This video demonstrates the *on-demand* separation of span80 stabilized water-in-hexadecane emulsion driven by gravity. A liquid column of water-in-hexadecane emulsion is retained above the membrane before applying an electric field. The water-in-hexadecane emulsion is demulsified into the water-rich and the hexadecane-rich phases when a voltage $V \approx 2.0$ kV is applied. After the onset of demulsification, water-rich permeate passes through, while hexadecane-rich retentate is retained above the membrane. Water is dyed blue and hexadecane is dyed red.

Movie S5. This video demonstrates the continuous separation of span80 stabilized water-in-hexadecane emulsion that is triggered *on-demand*. On continuously applying a voltage $V \approx 2.0$ kV, at steady state, water-rich permeate passes through the membrane module at the bottom, while hexadecane-rich permeate passes through the hydrophobic and oleophilic membrane on the sidewall. Water is dyed blue and hexadecane is dyed red.